

A flexible large-area triboelectric generator by low-cost roll-to-roll process for location-based monitoring



Xiaoliang Cheng, Yu Song, Mengdi Han, Bo Meng, Zongming Su, Liming Miao,
Haixia Zhang*

National Key Laboratory of Science and Technology on Micro/Nano Fabrication, Institute of Microelectronics, Peking University, Beijing 100871, China

ARTICLE INFO

Article history:

Received 18 November 2015
Received in revised form 31 May 2016
Accepted 31 May 2016
Available online 4 June 2016

Keywords:

Triboelectric generator
Large-area energy harvester
Power floor
Location-based monitoring

ABSTRACT

This paper discusses a flexible large-area power floor developed based on the effect of triboelectrification and electrostatic induction. Facilitated by a simple roll-to-roll fabrication method, this device can be fabricated at a very low cost of \$2/m² with large-area micro patterns. As a normal adult walks across the floor, it can produce more than 480V peak voltage and over 75 μA peak current. The obtained peak instantaneous power was about 4.6 mW. It also showed favorable charging ability, as demonstrated by charging a 1 μF capacitor to 1.6 V in one step, corresponding to a surface charge density of 53.3 μC/m². The spacer distance was systematically investigated and optimized by finite element simulation method. Therefore, this device can produce a pressure sensitivity of 7.1 V/KPa in the pressure range from 2.5 KPa to 30 KPa experimentally, which is about 4.67 times higher than similar devices using the same mechanism. A novel triboelectric generator (TEG) array was proposed based on this large-area TEG (LTEG) for position monitoring. Integrated with the function of power generation and position monitoring, the proposed device is directly applicable to LED-based alarm signals. Generated electricity can be stored in capacitor for use by low-power electronics. Employing a simple signal-processing circuit, the generated signal can also be used to control certain house-hold appliances. In effect, the proposed LTEG has considerable potential for application in harvesting walking energy as well as monitoring human motions.

© 2016 Elsevier B.V. All rights reserved.

1. Introduction

Energy crises are a well-accepted and increasingly serious worldwide problem, and researchers are responding by making concerted effort to establish new methods of harvesting energy. Rapid advancements in energy harvesting technology have created alternatives to traditional batteries, for example, to supply power for micro-scale devices [1,2]. Among all types of energy alternatives that exist naturally in our environment, mechanical energy has attracted particular research attention [3,4]. In the last ten years, many attempts have been made to convert mechanical energy from our environment to usable energy for wireless sensor nodes and wearable electronics [5–7]. The most commonly adopted mechanisms are electromagnetic induction [8], electrostatic induction [9–11] and piezoelectric effect [12], while different mechanisms show particular advantages to specific applications.

TEG, as one type of electrostatic energy harvester, has undergone rather extensive research in recent years [13–17]. It has garnered much interest due to its high power density and power conversion efficiency [14,17] as well as its potential applications in wireless systems [18,19], portable electronics [20,21], active sensors [22–24] and biomedical systems [25]. By far, these devices' output performance is mainly enhanced by nano, micro, or micro-nano dual-sized structures [20,25–27]. In many cases, such as power floor, an LTEG is preferred. Unfortunately, these structures are too challenging to fabricate and too expensive for large-area applications. Furthermore, work remains to be done to effectively fabricate TEG arrays suited to large areas with sufficient sensitivity to accurately detect motion.

This paper presents an LTEG-based power floor that converts human energy (i.e., walking) into electricity. We employed a roll-to-roll method to fabricate main structure from commercially available, low-cost material. High-output performance was obtained under one's normally walking on it. Output performance at varying spacer distances and pressures were systematically analyzed after a series of experiments; we found that by optimizing the spacer distance, a high sensitivity between voltage and pressure

* Corresponding author.

E-mail address: zhang-alice@pku.edu.cn (H. Zhang).

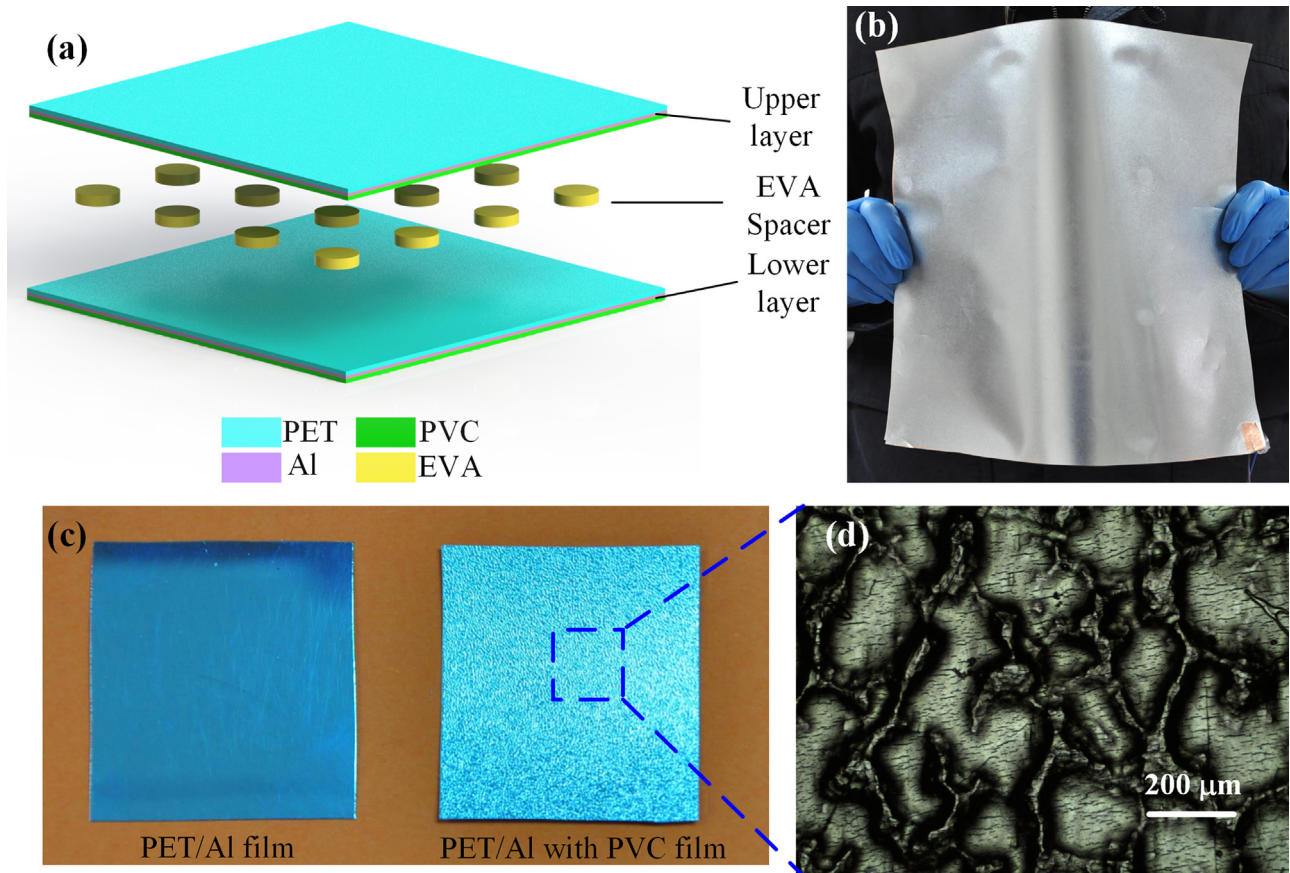


Fig. 1. Schematic diagram of the LTEG. (a) Explosive 3D view of this device. (b) Photograph of the LTEG to exhibit its flexibility. (c) Comparison of photographs of the PET/Al film with PET/Al/PVC film. (d) Microphotograph of the surface structure of PVC film.

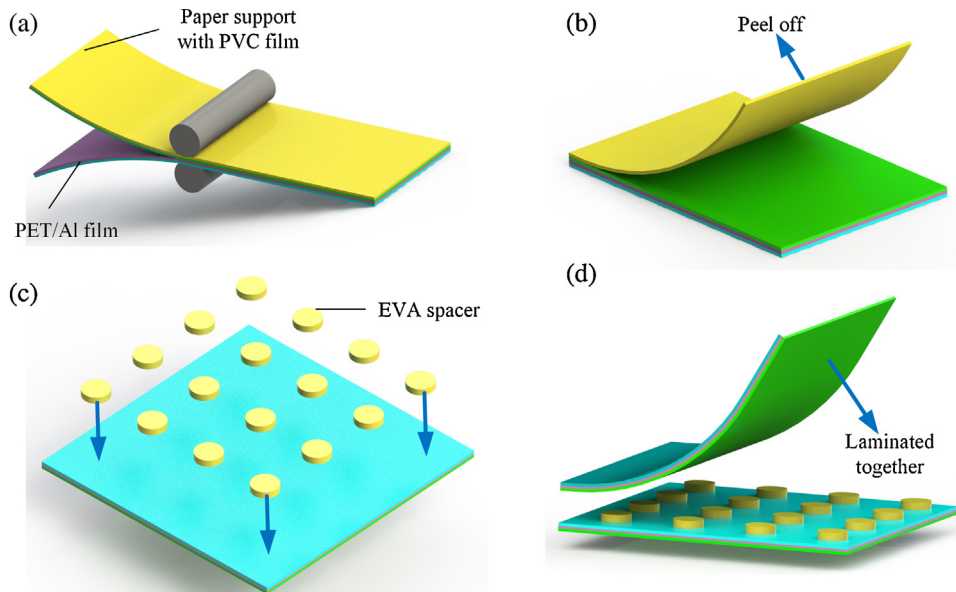


Fig. 2. Fabrication process of the LTEG. (a) Roll-to-roll laminating PET/Al film with PVC film together. (b) Peeling off the protecting layer of PVC. (c) Placing the EVA spacers array. (d) Laminating two layers together.

was obtainable. The device also showed high charging ability and capability to drive commercial LEDs, suggesting that it can serve as a smart floor for detecting motion and target locations to produce alarm signals.

2. Design of the device

Fig. 1a shows the explosive 3D diagram of the proposed LTEG. Both the upper and the lower part consist of a 100 μm polyethylene terephthalate (PET) film, a 100 nm aluminum (Al) layer on the

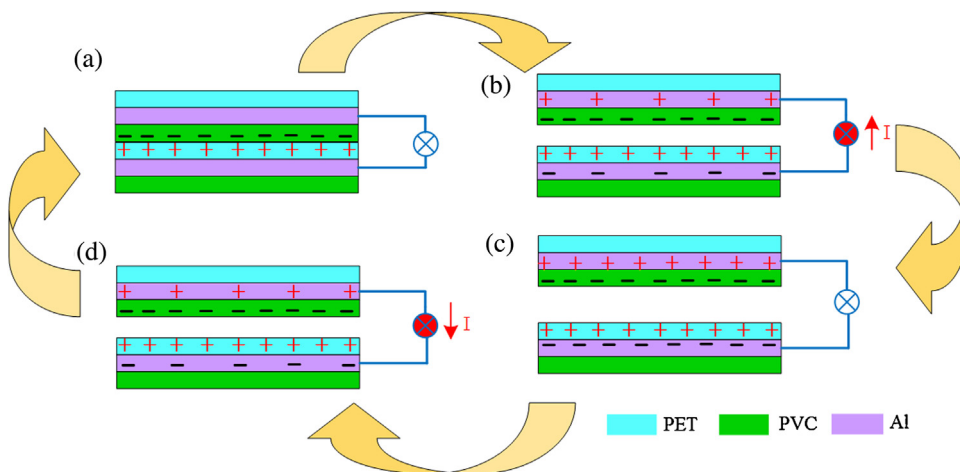


Fig. 3. Working principle of the LTEG. (a) Original state. PVC film and PET film contacts with each other, leading charges to separate. (b) Releasing state. Current flows from bottom electrode to top electrode to reach the electrostatic equilibrium. (c) Released state. Electrostatic equilibrium achieved. (d) Pressing state. Current flows back.

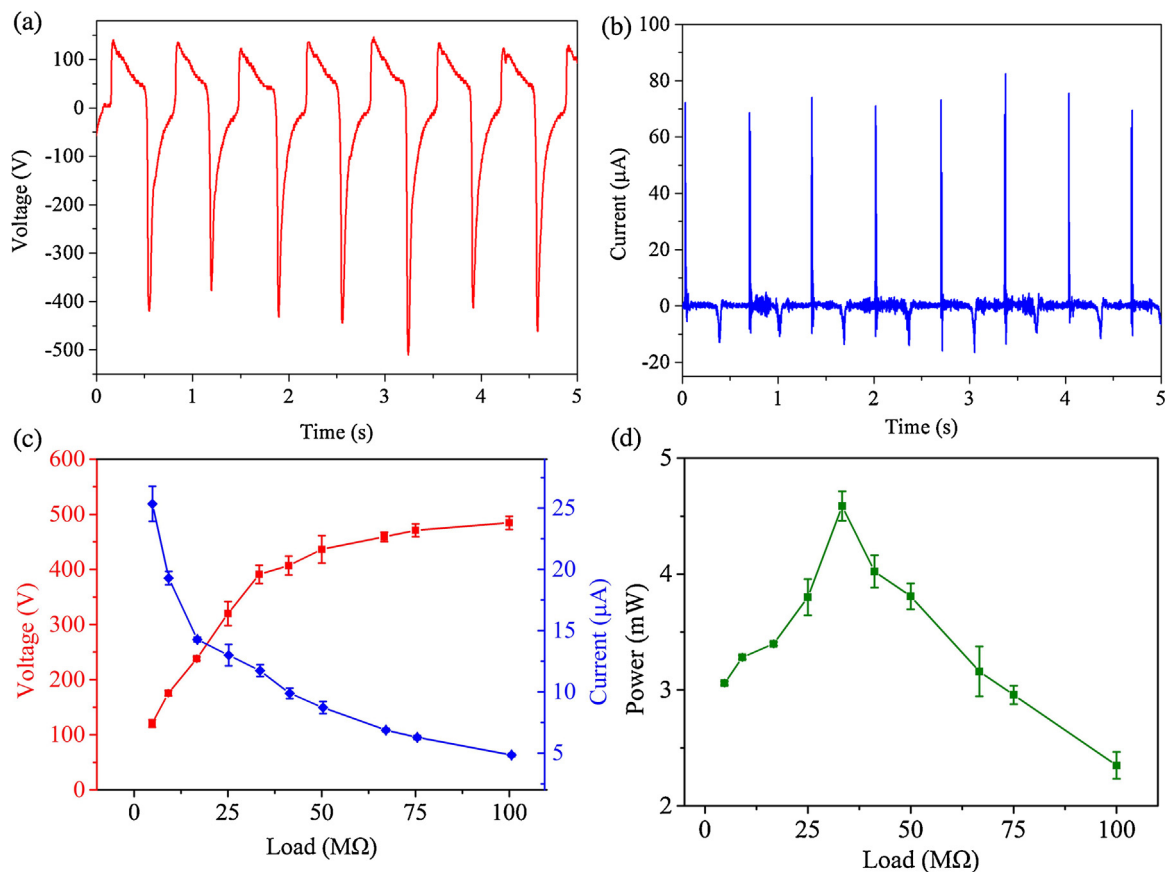


Fig. 4. (a) The output voltage waveform generated by an adult person walking on the floor. (b) The output current waveform generated by an adult person walking on the floor. (c) The generated output voltage increases with the load while the current decreases with the load. (d) The maximum generated instantaneous power under different loads.

PET surface as the electrode, and a 100 μm surface-microstructured polyvinyl chloride (PVC) film. Both of the PVC film of upper part and PET film of lower part serve as the contact layer to exploit their unique properties and ability to attract electrons in triboelectric series [28]. The as-fabricated device, with dimensions of about 30 cm \times 30 cm \times 3.5 mm is shown in Fig. 1b. The entire device exhibited good flexibility. A commercially available matte PVC film was laminated on PET/Al film to increase the surface roughness for enhanced triboelectric output (Fig. 1c). In addition to enhanc-

ing the surface roughness, the PVC film also formed a protective layer for the Al electrode, allowing the LTEG to work stably even in harsh environments. A microphotograph of the micro pattern on PVC film is shown in Fig. 1d. The dimension of micro patterns is at the hundred microns' level.

The fabrication process of this LTEG is diagrammed in Fig. 2. Firstly, we used a roll-to-roll method to form the large-area pattern, i.e., to laminate the PET/Al and matte PVC film together as shown in Fig. 2a. The protection layer of PVC film was peeled off to expose the micro-

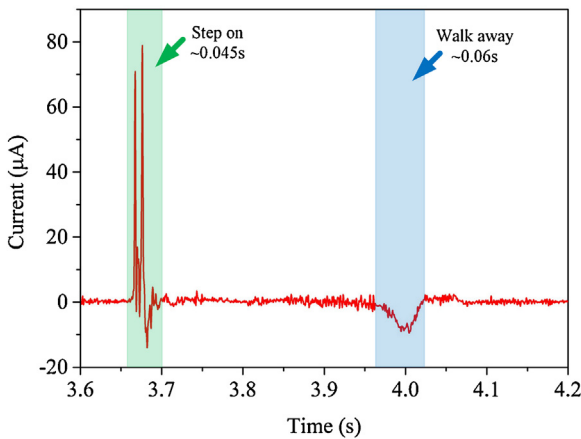


Fig. 5. The response times of LTEG when a person steps on and walks away from it.

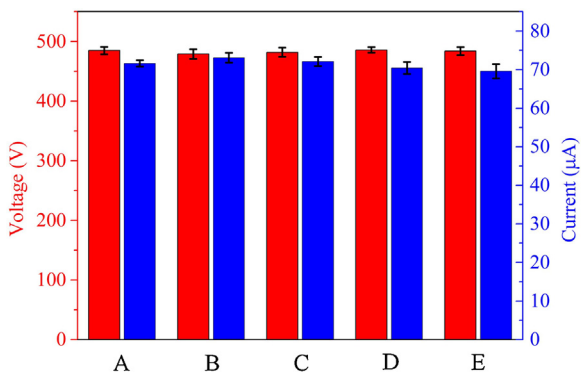


Fig. 6. The comparisons of output voltage and current generated by an adult person walking on different parts of the floor (i.e. A, B, C, D, E, which represents four corners and central part of the LTEG, respectively.).

patterned surface (Fig. 2b). Next, spacers made of Ethylene vinyl-acetate copolymer (EVA) foam were manually placed in an array and adhered to the PVC film (Fig. 2c). Finally, the upper layer was laminated together with the lower layer and EVA spacers to form the LTEG as shown in Fig. 2d. The utilization of EVA spacers fixed the gap distance between two layers at 3 mm, which ensured high charge transfer efficiency [29]. The EVA spacers were also able to fix the upper part and lower part together, making the entire device stronger and more stable.

3. Operating principle

Fig. 3 diagrams the operating principle of the LTEG. Once a person steps on the power floor, two parts of the device will get into contact with each other as shown in Fig. 3a. Due to PVC film's stronger ability to attract electrons, negative charges will accumulate on the surface of PVC film in the upper part, while the PET film in lower part will accumulate the same amount of charges with opposite polarity. Meanwhile, an elastic energy would be stored in this device due to the deformation of the structure. Afterwards, when the person walks down the power floor, two parts will be separated under the elastic force and revert instantaneously to their original shape. This would cause the opposite polar charges' separation at the same time and produce an electric potential difference in the upper and lower electrodes in Fig. 3b. This potential difference will drive the current from the lower electrode through the load to the upper electrode in order to reach the electrostatic equilibrium in Fig. 3c. Similarly, when the PET film gets closer with the PVC film due to outer mechanical force, the electric potential difference

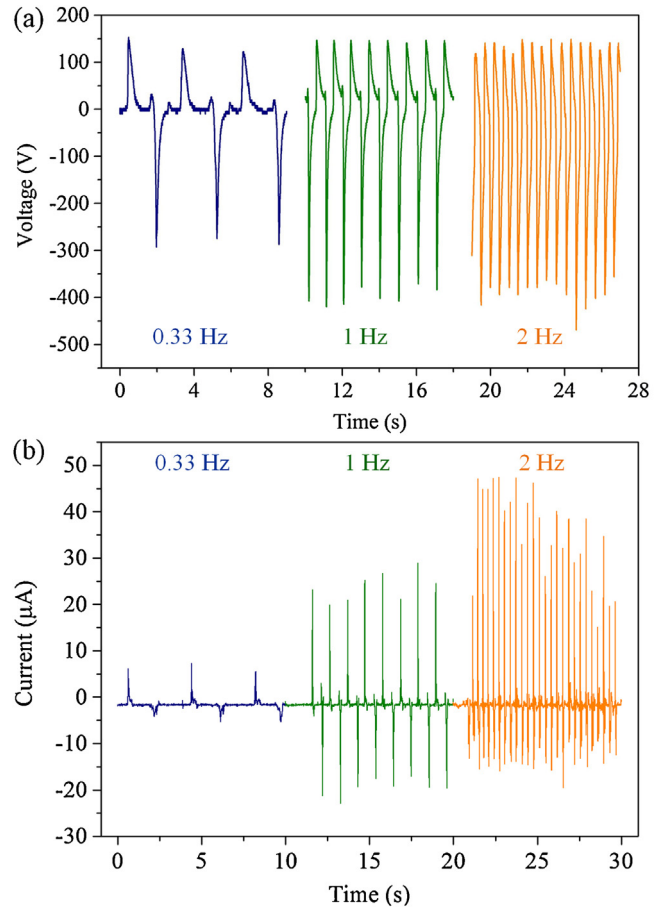


Fig. 7. (a) The output voltage as a function of the walking frequency. (b) The output current as a function of the walking frequency.

will decrease gradually caused by the reduced distance between the opposite polar charges. This makes the electrons transferring from the lower electrode to the upper electrode to form an opposite direction current. Finally, the PET film of the lower part will touch the PVC film of the upper part closely, and no electrons flow between two electrodes. As a result, when people walk on the triboelectric power floor, alternating current will be generated between the two electrodes.

4. Results and discussion

4.1. Output characterization

The output performance of LTEG was characterized by a person normally walking on its surface. The walking frequency was about 1.5 Hz for the characterization of the electric performance. Different frequencies were generated via a person walking at different speeds. The walking frequency was controlled by reading the signal of electric output from LTEG. An electronic scale was placed under the LTEG to display the total force applied to it in real time. When comparing the performances of LTEG under different frequencies, the maximum force was kept almost constant (i.e., the pressure was 25 KPa). The output voltage was measured via an oscilloscope (Agilent DSO-X 2014A) with an input impedance of 100 MΩ (HP 9258). And the output current was amplified by a SR570 low noise current amplifier from Stanford Research systems.

Fig. 4a–b shows the output voltage and current waveform generated by an adult person walking across the LTEG. As discussed in the operating principle, the produced electricity was an alter-

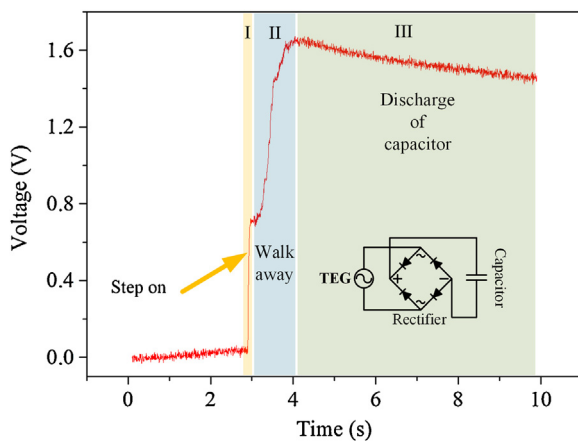


Fig. 8. The charging curve for a $1 \mu\text{F}$ capacitor during one step.

nating signal. The average maximum value of output voltage was measured above 480 V while each peak wave had a long duration time. The average maximum output current was about $75\text{ }\mu\text{A}$, corresponding to a surface current density of about $0.5\text{ }\mu\text{A}/\text{cm}^2$ (considering the area of experimenter's foot). The influence of the microstructures on the PVC film to the electric performance was shown in Fig. S1 (Supplementary information). Compared to an LTEG without microstructures, the voltage of the LTEG with microstructures increased about 140%. To obtain its equivalent resistance, the device's output was measured by varying the resistances. As shown in Fig. 4c, the output voltage increased with the load while the current simultaneously decreased. The maximum output power was about 4.6 mW when the resistor was $33.3\text{ M}\Omega$, as plotted in Fig. 4d, resulting in a power density of about 0.3 W/m^2 . Considering that the total cost of the LTEG was about two U.S. dollar per square meter, the cost per unit of power is approximately $\$6.67/\text{W}$. The method proposed here is one of the cheapest possible for producing this large of a TEG.

Fig. 5 shows an enlarged image of the short-circuit current. Because the current in short circuit state is synchronous with the movement of the device to reach the electrostatic equilibrium, the current waveform can be used to calculate the contact and separation time of the two layers of the LTEG, which greatly affects the device's performance. The contact time was about 0.045 s , which was directly related to the experimenter's walking speed. After walking away from the LTEG, the two layers separated to recover their initial shape. The separation time was about 0.06 s , which approximated to the contact time, and was mainly determined by the mechanical structure of LTEG. Taking average walking frequency (much lower than 10 Hz) into account, this separation time is adequate.

For any large-area device such as ours, it is important (but difficult) to ensure it can produce consistent outputs. The spacers must be placed uniformly in different parts of the device. As illustrated in Fig. 6, the peak output voltage and current of different parts (A, B, C, D, E, which represent four corners and center of the LTEG, respectively.) were measured. The peak output voltages of these five parts were about 485 V , 479 V , 482 V , 486 V , and 484 V , respectively, corresponding to a maximum difference of 1.4%. And the peak output currents were about $71\text{ }\mu\text{A}$, $73\text{ }\mu\text{A}$, $72\text{ }\mu\text{A}$, $70\text{ }\mu\text{A}$, and $69\text{ }\mu\text{A}$, respectively, the maximum difference of currents was less than $4\text{ }\mu\text{A}$, about 5.4%.

Walking speed is another factor affecting the performance of LTEG, as plotted in Fig. 7. The output voltage reached its maximum value at walking speed above 1 Hz , while its duration became shorter with each cycle as walking speed increased. The current also showed an increasing trend with the walking speed, and

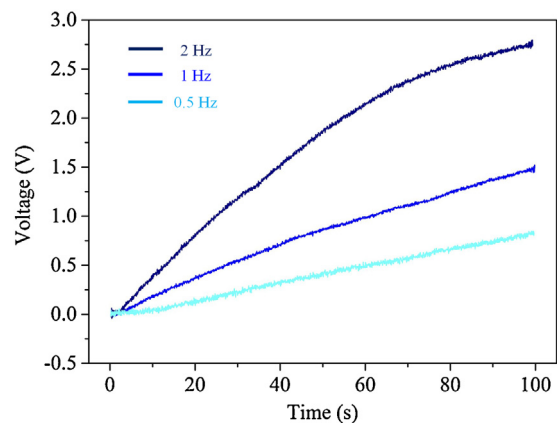


Fig. 9. Charging curve for a $50 \mu\text{F}$ capacitor by generated electricity as a function of walking speed.

reached maximum value at walking speed of 2 Hz . This difference in relationship to frequency between voltage and current can be attributed to the different loads connected with the LTEG. A $100\text{ M}\Omega$ probe was used to obtain the voltage signal, which made the charge transfer slower and affected the point at which maximum value was reached compared to the current being measured with a $1\text{ }\Omega$ probe. Accordingly, increase in frequency created higher charge flow rate, resulting in a higher current.

4.2. Charging ability

The output energy should be stored first during practical application. Because the alternating current could not be stored directly, the electricity extracted from the device was rectified to direct current signal via a commercial full-wave rectifier bridge (DB107) as shown in Fig. 8. Then it was used to charge a $1 \mu\text{F}$ capacitor at up to 1.6 V in one step. The calculated transferred charge in one step was thus about $1.6\text{ }\mu\text{C}$, corresponding to a surface charge density of $53.3\text{ }\mu\text{C/m}^2$. The charging curve can be divided into three stages. When a person stepped on the LTEG, its two layers were brought into contact to produce the first-stage charging curve. Afterwards, the capacitor was charged to 1.6 V as the person walked across the floor. Finally, the capacitor discharged as a result of the limited impedance of the probe.

To test the device's long-term charging ability, we used it to charge a $50 \mu\text{F}$ capacitor as shown in Fig. 9. The capacitor was charged to 0.83 V under the frequency of 0.5 Hz within 100 s . Charging ability increased as frequency increased due to the greater number of charge transfer cycles caused by increase in frequency. When frequency reached 2 Hz , the capacitor could be charged to 2.75 V within 100 s .

4.3. For location-based monitoring

As mentioned above, the triboelectric generator is an active pressure sensor with high sensitivity [13]. When the power floor is used as a security monitoring sensor, avoiding false triggering is a crucial consideration. The spacer distance is a key factor that affects the device's sensitivity and thus its susceptibility to false triggers. We used finite element method (FEM) simulation to determine the appropriate spacer distance. During the simulation, we assumed a small object (e.g., a cat) produced a 2.5 KPa pressure to the power floor while a person generated a pressure of 25 KPa . When the distance and pressure were 7 mm and 25 KPa , respectively, the simulation result was as shown in Fig. 10a. The maximum deformation was 4 mm , which was larger than the thickness of spacer (3 mm), creating deformation that ensured contact between the

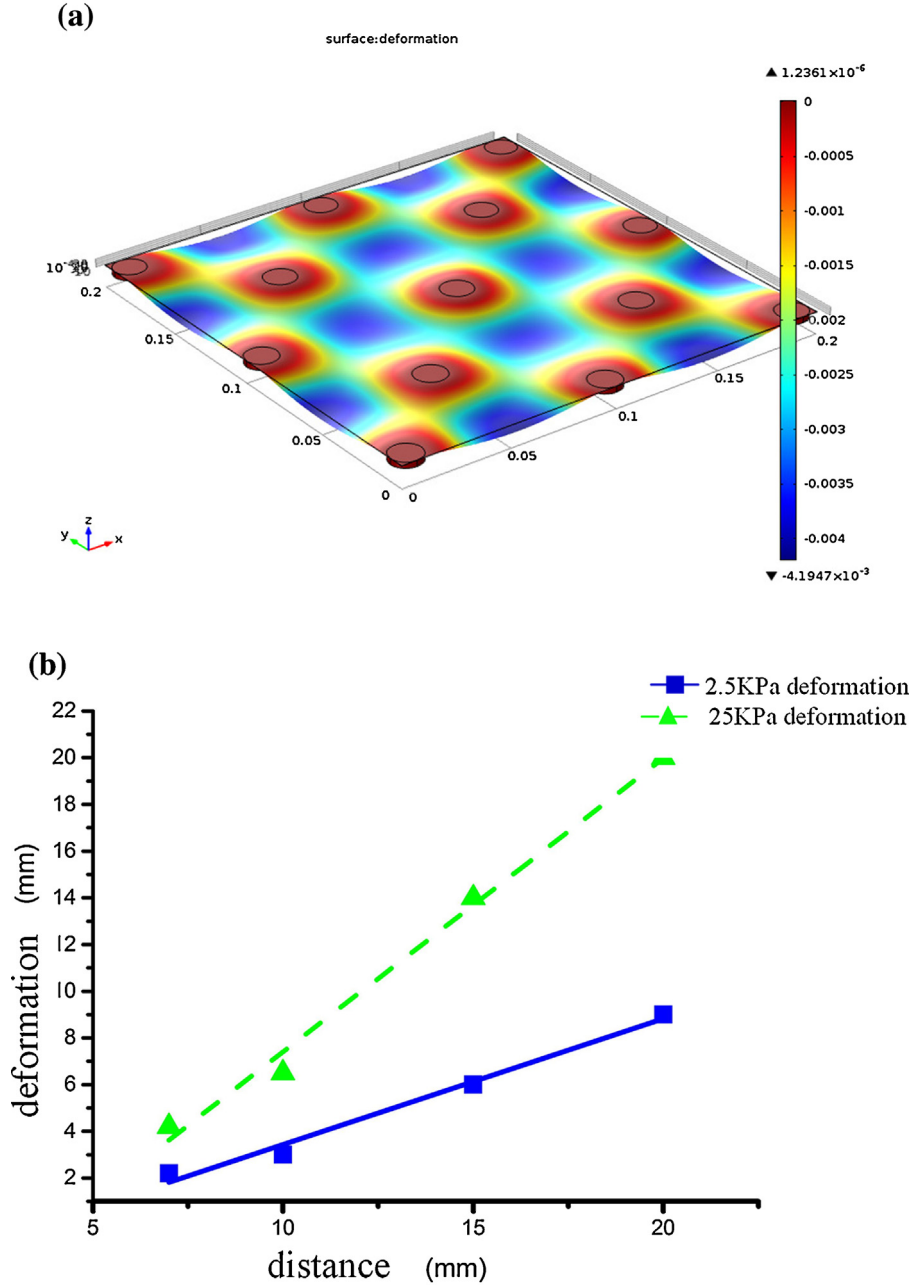


Fig. 10. Simulated deformations of the power floor under different spacer distances.

two films. The deformations under different distances are shown in Fig. 10b. The maximum deformation was proportional to the spacer array distance when the pressure was fixed, and when the distance was 7–10 mm, a 2.5 KPa pressure produced a deformation less than 3 mm while a deformation more than 4 mm was achieved under 25 KPa. According to these results, a 7–10 mm spacer distance would prevent false triggering during practical use. And in this work, the spacer distance was fixed at 10 mm for all subsequent experiments.

The sensitivity of the LTEG was further investigated by experimentally testing the output voltages under different pressures. As shown in Fig. 11, voltage increased linearly as pressure increased from 2.5 KPa to 30 KPa. Sensitivity can be defined as follows:

$$S = \frac{\delta V_{\max}}{\delta P} \quad (1)$$

where V_{\max} is the generated maximum voltage by LTEG and P is the applied pressure. We found that the sensitivity of the sensor was 7.1 V/KPa in the pressure range from 2.5 KPa to 30 KPa. Notably, this sensitivity was about 4.67 times higher than other TEG-based pressure sensor (< 1.52 V/KPa) as reported by previous work [30–33], due to the fact that the EVA spacers moved the most sensitive pressure region of TEG from very low pressure to the region generated by an average adult person walking. As discussed above, this region can be further adjusted by controlling the spacer distance.

To test the device's target monitoring capability, we fabricated a novel LTEG array and integrated it into a matrix as diagrammed in Fig. 12. As opposed to the basic structure of the LTEG described above, both the upper layer and the lower layer were designed as individual channels which worked in the single-electrode-mode. All the channels were measured with respect to an individual reference via a $100 \text{ M}\Omega$ probe. Because the materials of upper layer

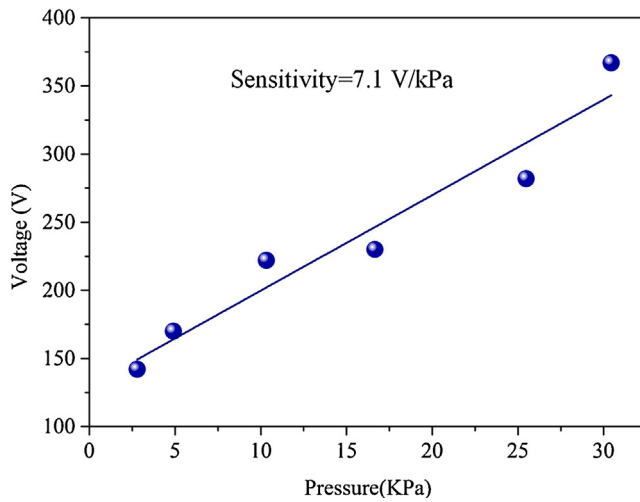


Fig. 11. Experimentally obtained voltage from the LTEG as a function of applied pressure by a person at a constant walking frequency of 1.5 Hz.

and lower layer have opposite polarity, their output signals were in opposite directions. The specific position of a given target can be observed by simultaneously obtaining output signals from the unit.

Fig. 13a depicts a target monitoring test run in which a person stepped on the top left corner of the units shown in Fig. 12. The channel 1 and channel 3 produced signals simultaneously with opposite direction to show the person's location. The signals from channel 2 and channel 4 were regarded as noise, and the signal to noise (SNR) ratio for this monitoring sensor array could be calculated as follows:

$$SNR = \left(\frac{A_{signal}}{A_{noise}} \right)^2 \quad (2)$$

where A_{signal} is the amplitude of the required signal and A_{noise} is the amplitude of noise. The amplitudes of signals from the channels from 1 to 4 were 35.4 V, 4.5 V, 11.6 V, and 3.7 V. By plugging these values into Eq. (2), the SNR for channel 1 and channel 3 were calculated as 61.9 and 9.9, respectively.

5. Demonstration

By integrating the features of power generation and position monitoring, the LTEG shows attractive potential as an active sensor

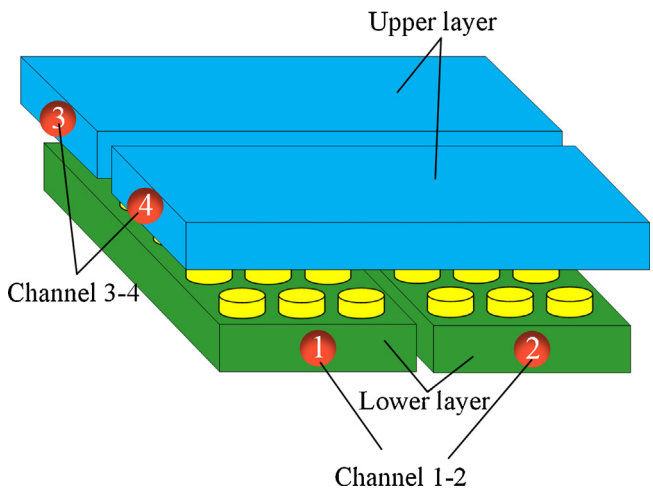


Fig. 12. Schematic diagram of the matrix connection method of the LTEGs for location based monitoring.

for smart home systems. First, through a full wave rectifier, it can directly power several LEDs (which can serve as an alarm signal) once a person steps onto the device (Fig. 14a). Second, the device was designed with an electric circuit for triggering the alarm system or for powering household appliances (Fig. 14b). In the proposed system, the generator serves as a sensor that generates an alarm signal, then through a simple signal-processing circuit [34], the alarm signal either sounds an alarm or powers an appliance assisted by an external power supply. The LTEG was placed on the ground to test its ability to detect human motion with an alarm. Once the experimenter stepped on the LTEG, the alarm sounded and flashed. In a similar way, a mini fan was also employed to represent a household appliance in the smart house. The mini fan would be turned on if a person stepped on it. In terms of practical application, the LTEG could be placed under an entryway carpet to turn on lights or start other appliances when the homeowner steps through the front door (or could sound an alarm if an intruder stepped into the home). The power generated by the LTEG can also be stored for subsequent use by low-consumption electronic devices.

6. Conclusions

In this study, an LTEG based power floor was designed, fabricated, and optimized. By utilizing a roll-to-roll fabrication method

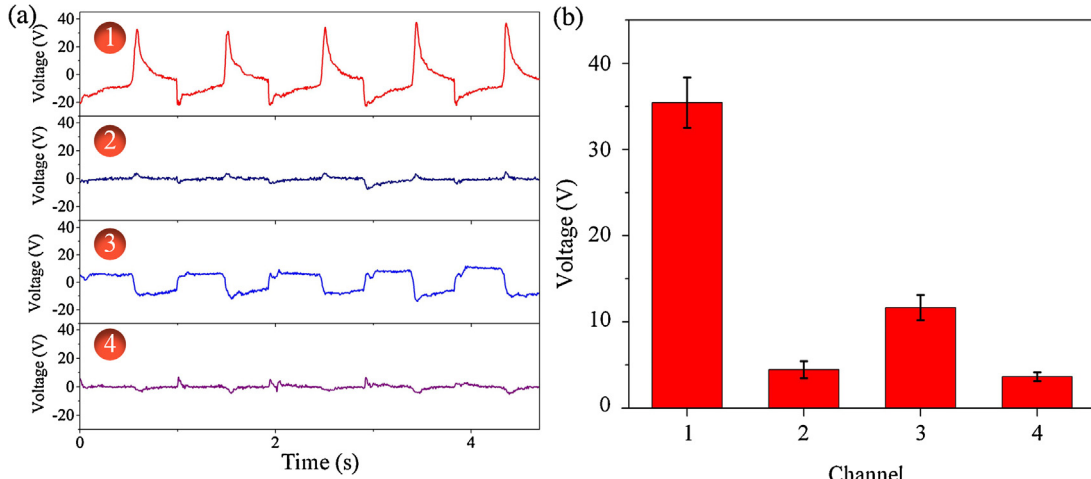


Fig. 13. (a) The experimentally obtained signals from four channel of the matrix-LTEG and (b) the comparisons of amplitude of these signal.

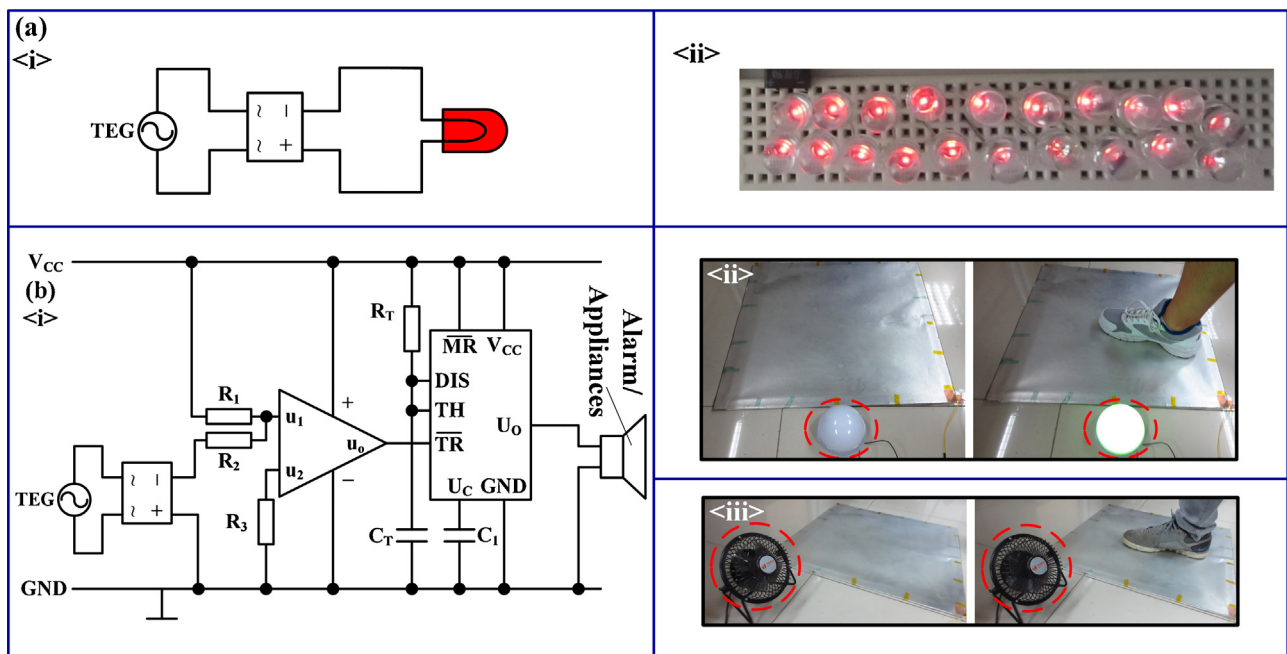


Fig. 14. (a) Demonstration of using the LTEG as a self-powered warning sensor. (b) Electric circuit for triggering the alarm system or appliances by the LTEG. An alarm system was triggered once a person step on the LTEG <i><ii></i>. (c) A mini fan was opened automatically once a person step on the LTEG <i><iii></i>.

and commercially available material, the floor was built with large-area micro patterns at a very low price. As an average adult walked across the floor, more than 480 V output voltage and over 75 μ A output current were obtained. The peak instantaneous output power was about 4.6 mW with an equivalent resistance of about 33.3 M Ω . The device also showed a high charging ability, generating 1.6 μ C transferred charge during one step and charging a 50 μ F capacitor to 2.75 V in only 100 s. After optimizing the distance between its EVA spacers, the device showed very high sensitivity (7.1 V/KPa) in the pressure range from 2.5 KPa to 30 KPa. A novel TEG array was designed to monitor target positons with high SNR. Due to its high output performance, the generator was able to power 20 red LEDs as an average adult walked across the floor. By employing a simple signal-processing circuit, the electricity generated from the device was able to be used to switch some house-hold appliances. Taken together, the results presented above suggest that the proposed LTEG shows considerable potential as an active sensor for security monitoring or smart home purposes.

Acknowledgements

This work is supported by the National Natural Science Foundation of China (Grant No. 61176103 and 91323304), the National Hi-Tech Research and Development Program of China ("863" Project) (Grant No. 2013AA041102), and the National Ph. D. Foundation Project (Grant No. 20110001110103) and the Beijing Natural Science Foundation of China (Grant No. 4141002).

Appendix A. Supplementary data

Supplementary data associated with this article can be found, in the online version, at <http://dx.doi.org/10.1016/j.sna.2016.05.051>.

References

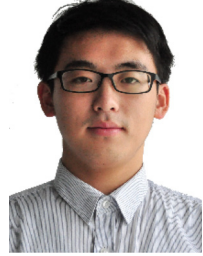
- [1] Y. Hu, L. Lin, Y. Zhang, Z.L. Wang, Replacing a battery by a nanogenerator with 20V output, *Adv. Mater.* 24 (2012) 110–114.
- [2] J. Matiko, N. Graham, S. Beeby, M. Tudor, Review of the application of energy harvesting in buildings, *Meas. Sci. Technol.* 25 (2014) 012002.
- [3] X. Dai, Y. Wen, P. Li, J. Yang, M. Li, Energy harvesting from mechanical vibrations using multiple magnetostrictive/piezoelectric composite transducers, *Sens. Actuators A* 166 (2011) 94–101.
- [4] G.K. Ottman, H.F. Hofmann, G.A. Lesieutre, Optimized piezoelectric energy harvesting circuit using step-down converter in discontinuous conduction mode Power Electronics, *IEEE Trans.* 18 (2003) 696–703.
- [5] S.P. Beeby, M.J. Tudor, N. White, Energy harvesting vibration sources for microsystems applications, *Meas. Sci. Technol.* 17 (2006) R175.
- [6] H. Zhang, X.-S. Zhang, X. Cheng, Y. Liu, M. Han, X. Xue, et al., A flexible and implantable piezoelectric generator harvesting energy from the pulsation of ascending aorta: *in vitro* and *in vivo* studies, *Nano Energy* 12 (2015) 296–304.
- [7] Y. Qin, X. Wang, Z.L. Wang, Microfibre–nanowire hybrid structure for energy scavenging, *Nature* 451 (2008) 809–813.
- [8] M. Han, Z. Li, X. Sun, H. Zhang, Analysis of an in-plane electromagnetic energy harvester with integrated magnet array, *Sens. Actuators A Phys.* 219 (2014) 38–46.
- [9] Y. Sakane, Y. Suzuki, N. Kasagi, The development of a high-performance perfluorinated polymer electret and its application to micro power generation, *J. Micromech. Microeng.* 18 (2008) 1023–1029.
- [10] Y. Suzuki, Recent progress in MEMS electret generator for energy harvesting, *Ieej Trans. Elect. Electron. Eng.* 6 (2011) 101–111.
- [11] K. Tao, J. Miao, W.L. Sun, X. Hu, Sandwich-structured two-dimensional MEMS electret power generator for low-level ambient vibrational energy harvesting, *Sens. Actuators A Phys.* 228 (2015) 95–103.
- [12] Y.B. Jeon, R. Sood, J.H. Jeong, S.G. Kim, MEMS power generator with transverse mode thin film PZT, *Sens. Actuators A Phys.* 122 (2005) 16–22.
- [13] F.R. Fan, L. Lin, G. Zhu, W. Wu, R. Zhang, Z.L. Wang, Transparent triboelectric nanogenerators and self-powered pressure sensors based on micropatterned plastic films, *Nano Lett.* 12 (2012) 3109–3114.
- [14] G. Zhu, Z.H. Lin, Q. Jing, P. Bai, C. Pan, Y. Yang, et al., Toward large-scale energy harvesting by a nanoparticle-enhanced triboelectric nanogenerator, *Nano Lett.* 13 (2013) 847–853.
- [15] F.A. Hassani, C. Lee, A triboelectric energy harvester using low-cost, flexible, and biocompatible ethylene vinyl acetate (EVA), *J. Microelectromech. Syst.* 24 (2015) 1338–1345.
- [16] L. Dhakar, F.E.H. Tay, C. Lee, Development of a broadband triboelectric energy harvester with su-8 micropillars, *J. Microelectromech. Syst.* 24 (2015) 91–99.
- [17] G. Zhu, J. Chen, T. Zhang, Q. Jing, Z.L. Wang, Radial-arrayed rotary electrification for high performance triboelectric generator, *Nat. Commun.* 5 (2014) 3426.
- [18] W. Tang, T. Zhou, C. Zhang, F.R. Fan, C.B. Han, Z.L. Wang, A power-transformed-and-managed triboelectric nanogenerator and its applications in a self-powered wireless sensing node, *Nanotechnology* 25 (2014) 225402.
- [19] S. Wang, X. Mu, Y. Yang, C. Sun, A.Y. Gu, Z.L. Wang, Flow driven triboelectric generator for directly powering a wireless sensor node, *Adv. Mater.* 27 (2014) 240–248.
- [20] S. Wang, L. Lin, Z.L. Wang, Nanoscale triboelectric-effect-enabled energy conversion for sustainably powering portable electronics, *Nano Lett.* 12 (2012) 6339–6346.

- [21] X. Cheng, B. Meng, X. Zhang, M. Han, Z. Su, H. Zhang, Wearable electrode-free triboelectric generator for harvesting biomechanical energy, *Nano Energy* 12 (2015) 19–25.
- [22] B. Meng, W. Tang, Z.-h. Too, X. Zhang, M. Han, W. Liu, et al., A transparent single-friction-surface triboelectric generator and self-powered touch sensor, *Energy Environ. Sci.* 6 (2013) 3235.
- [23] B. Meng, X. Cheng, M. Han, H. Chen, F. Zhu, H. Zhang, Triboelectrification based active sensor for polymer distinguishing, micro electro mechanical systems (MEMS), 28th IEEE International Conference on, IEEE 2015 (2015) 102–105.
- [24] X. Cheng, B. Meng, M. Han, M. Shi, H. Zhang, Floor-based large-area triboelectric generator for active security monitoring, *Consumer Electronics (ICCE), IEEE International Conference on, IEEE 2015 (2015)* 581–582.
- [25] X.-S. Zhang, M.-D. Han, R.-X. Wang, B. Meng, F.-Y. Zhu, X.-M. Sun, et al., High-performance triboelectric nanogenerator with enhanced energy density based on single-step fluorocarbon plasma treatment, *Nano Energy* 4 (2014) 123–131.
- [26] M.L. Seol, J.W. Han, J.H. Woo, D.I. Moon, Comprehensive analysis of deformation of interfacial micro-nano structure by applied force in triboelectric energy harvester, *Electron Devices Meeting (IEDM), IEEE Int. (2014)* 8.3.1–8.3.4.
- [27] X. Cheng, B. Meng, X. Chen, M. Han, H. Chen, Z. Su, M. Shi, H. Zhang, Single-step fluorocarbon plasma treatment-induced wrinkle structure for high-performance triboelectric nanogenerator, *Small* 12 (2016) 229–236.
- [28] A.F. Diaz, A semi-quantitative tribo-electric series for polymeric materials: the influence of chemical structure and properties, *J. Electrostat.* 62 (2004) 277–290.
- [29] S. Niu, S. Wang, L. Lin, Y. Liu, Y.S. Zhou, Y. Hu, et al., Theoretical study of contact-mode triboelectric nanogenerators as an effective power source, *Energy Environ. Sci.* 6 (2013) 3576.
- [30] L. Lin, Y. Xie, S. Wang, W. Wu, S. Niu, X. Wen, Z.L. Wang, Triboelectric active sensor array for self-powered static and dynamic pressure detection and tactile imaging, *ACS Nano* 7 (2013) 8266–8274.
- [31] J. Luo, F.R. Fan, T. Zhou, W. Tang, F. Xue, Z.L. Wang, Ultrasensitive self-powered pressure sensing system, *Extreme Mech. Lett.* 2 (2015) 28–36.
- [32] H. Park, Y.R. Jeong, J. Yun, S.Y. Hong, S. Jin, S.J. Lee, G. Zi, J.S. Ha, Stretchable array for highly sensitive pressure sensors consisting of polyaniline nanofibers and au-coated polydimethylsiloxane micropillars, *ACS Nano* 9 (2015) 9974–9985.
- [33] S.K. Park, H. Kim, M. Vosgueritchian, S. Cheon, H. Kim, et al., Stretchable energy-harvesting tactile electronic skin capable of differentiating multiple mechanical stimuli modes, *Adv. Mater.* 26 (2014) 7324–7332.
- [34] M. Han, B. Yu, G. Qiu, H. Chen, Z. Su, M. Shi, et al., Electrification based devices with encapsulated liquid for energy harvesting, multifunctional sensing, and self-powered visualized detection, *J. Mater. Chem. A* 3 (2015) 7382–7388.

Biographies



Xiaoliang Cheng received the B.S. degree from the University of Electronic Science and Technology of China, Chengdu, in 2014. He is currently pursuing the Ph.D. degree at the National Key Laboratory of Nano/Micro Fabrication Technology, Peking University, Beijing, China. His research interests mainly include design and fabrication of nanogenerator and mechanical energy harvester.



Yu Song received the B.S. degree in Electronic Science & Technology from Huazhong University of Science and Technology, China, in 2015. He is currently pursuing the Ph.D. degree at the National Key Laboratory of Nano/Micro Fabrication Technology, Peking University, Beijing, China. He majors in MEMS and his research is focusing on supercapacitors and energy harvester.



Bo Meng received his B.S. degree in Electronic Science & Technology from Huazhong University of Science and Technology, China in 2011. He is a Ph.D. candidate in National Key Lab of Nano/Micro Fabrication Technology at Peking University, China. He majors in MEMS and his research interests are energy harvester and SiC MEMS.



Mengdi Han received the B.S. degree in Electronic Science & Technology from Huazhong University of Science and Technology, China, in 2012. He is currently pursuing the Ph.D. degree at the National Key Laboratory of Nano/Micro Fabrication Technology, Peking University, Beijing, China. His research work is focusing on nanogenerator and MEMS sensors.



Zongming Su received the B.S. degree from the University of Science and Technology Beijing, in 2013. He is currently pursuing the Ph.D. degree at the National Key Laboratory of Nano/Micro Fabrication Technology, Peking University, Beijing, China. His research interests are: (1) micro&nano structure fabrication; (2) piezoelectric material and (3) energy harvesting.



Haixia (Alice) Zhang (SM'10) received the Ph.D. degree in mechanical engineering from Huazhong University of Science and Technology, Wuhan, China, 1998. She is currently a Professor with the Institute of Microelectronics, Peking University, Beijing, China. She joined the faculty of the Institute of Microelectronics in 2001 after finishing her post-doctoral research in Tsinghua University. Her research interests include MEMS design and fabrication technology, SiC MEMS, and micro energy technology. She has served on the General Chair of the IEEE NEMS 2013 Conference, the Organizing Chair of Transducers'11. As the Founder of the International Contest of Applications in Network of things, she has been organizing this worldwide event since 2007. In 2006, she received the National Invention Award of Science and Technology.